

# Optimization of CO<sub>2</sub> Capture Efficiency in a Flue Gas Treatment System: Assessing the Impact of Flow Rates, Absorbent Concentrations, Nanoparticles, and Temperature

Maysoon Anwar Abdulla<sup>1,2\*</sup>, Abdelmottaleb ouederni<sup>2</sup>, Saad A. Jafar<sup>3</sup>

<sup>1,3</sup>*Petroleum and Gas Refining Engineering Department, College of Petroleum Processes Engineering, Tikrit University, Iraq; E-mail: [mayanwar@tu.edu.iq](mailto:mayanwar@tu.edu.iq)*

<sup>2</sup>*University of Gabes, National School of Engineers of Gabes, Laboratory of Research Process Engineering and Industrial Systems, LR11ES54, Gabes, Tunisia.*

**Abstracts:** This study focuses on improving the efficiency of flue gas purification systems for carbon dioxide (CO<sub>2</sub>) capture. The researchers investigated various factors, including flow rates, absorbent concentrations, nanoparticles, and temperature, to optimize the CO<sub>2</sub> capture process. They conducted experiments using a polytetrafluoroethylene (PTFE) hollow fiber membrane contactor to separate CO<sub>2</sub> from nitrogen. The presence of titanium dioxide and silica nanoparticles in a potassium carbonate solution facilitated the separation process. The findings indicate that optimizing flow rates and absorbent concentrations can enhance CO<sub>2</sub> capture efficiency. The use of nanoparticles in the absorbent solution was found to improve material capture effectiveness. The study also revealed that higher temperatures contribute to increased CO<sub>2</sub> capture efficiency. The research aims to advance CO<sub>2</sub> capture techniques to mitigate the release of industrial greenhouse gases, particularly in flue gas treatment systems. The researchers determined optimal settings for CO<sub>2</sub> capture in these systems, emphasizing the importance of absorbent concentration for stability and absorption, as well as the role of nanoparticles in enhancing reaction kinetics and CO<sub>2</sub> collection. The objective of the analysis is to maximize removal efficiency, although specific lower and upper bounds and a target value were not provided. The proposed solution suggests specific values for the independent variables, including temperature, gas flow rate, liquid flow rate, and the concentrations of K<sub>2</sub>CO<sub>3</sub>, PZ, SiO<sub>2</sub>, and TiO<sub>2</sub>, to optimize CO<sub>2</sub> capture.

**Keywords:** CO<sub>2</sub> Capture, Flue Gas Treatment, Optimization, Flow Rates, Absorbent Concentrations, Nanoparticles, Temperature, Capture Efficiency, Greenhouse Gas Emissions, Industrial Processes.

## 1. INTRODUCTION

The utilization of potassium carbonate (K<sub>2</sub>CO<sub>3</sub>) for the adsorption of carbon dioxide (CO<sub>2</sub>) is a noteworthy and adaptable approach within the domain of carbon capture and storage (CCS) technologies. The significance of this lies in its capacity to alleviate the discharge of carbon dioxide into the atmosphere, thereby tackling climate change and diminishing emissions of greenhouse gases [1]. This methodology exhibits extensive utility across diverse domains and fields. The utilization of K<sub>2</sub>CO<sub>3</sub> for CO<sub>2</sub> absorption finds significant application in power generation facilities, particularly those that depend on non-renewable energy sources [2]. The process of K<sub>2</sub>CO<sub>3</sub> absorption involves capturing CO<sub>2</sub> from the flue gas emissions of power plants, thereby preventing its release into the atmosphere. This results in a reduction of the carbon footprint associated with the energy generation process. Furthermore, it has the potential to be utilized in sectors characterized by significant CO<sub>2</sub> emissions, such as the production of cement, steel, and chemicals. The benefits associated with the utilization of K<sub>2</sub>CO<sub>3</sub> for the purpose of CO<sub>2</sub> adsorption are significant as indicated in reference [4]. Primarily, potassium carbonate demonstrates a notable inclination towards CO<sub>2</sub>, facilitating proficient and potent sequestration of the gas. The significant absorption capacity exhibited by K<sub>2</sub>CO<sub>3</sub> renders it a desirable absorbent for CO<sub>2</sub> capture applications on a large scale. In addition, K<sub>2</sub>CO<sub>3</sub> is easily accessible and comparatively affordable, thereby enhancing its cost-efficiency in comparison to alternative absorbents. An additional benefit is the simplicity in renewing the K<sub>2</sub>CO<sub>3</sub> solution and reclaiming the trapped CO<sub>2</sub>, as stated in reference [5]. Upon subjecting the potassium bicarbonate solution to thermal energy, the carbon dioxide is liberated in its gaseous form, thereby facilitating its segregation and subsequent retention or application. The process of regeneration renders the absorbent reusable, thereby augmenting the overall efficiency and sustainability of the system designed for capturing CO<sub>2</sub> [6][7].

Nonetheless, the utilization of  $K_2CO_3$  for  $CO_2$  adsorption entails specific factors to be considered and possible drawbacks to be considered. An area of concern pertains to the energy demands associated with the process of regeneration. The process of liberating the sequestered  $CO_2$  from the solution necessitates an energy input, which, if sourced from fossil fuels, may counterbalance the ecological advantages accrued from  $CO_2$  capture. Consequently, the incorporation of renewable energy sources into the regeneration process is imperative to optimize the potential for carbon reduction [8]. An additional factor to be considered is the corrosive properties exhibited by solutions containing potassium carbonate. The corrosive potential of  $K_2CO_3$  due to its highly alkaline nature can result in equipment corrosion during the process of  $CO_2$  capture and storage [9]. The significance of potassium carbonate ( $K_2CO_3$ ) in carbon capture and storage (CCS) technologies is considerable, particularly in relation to its ability to adsorb  $CO_2$  [10]. Potassium carbonate is an alkaline compound possessing a strong attraction towards  $CO_2$ . The formation of a stable compound: the potassium bicarbonate ( $KHCO_3$ ) can occur through the reaction of  $CO_2$  and potassium, as evidenced by sources [5] [11].



The chemical process takes place within a liquid medium, commonly employing either an absorption column or a packed bed reactor. During this process, a  $CO_2$  stream is introduced to the  $K_2CO_3$  solution, facilitating the dissolution and chemical reaction of  $CO_2$  molecules with potassium carbonate. Consequently, the concentration of  $CO_2$  in the gas stream is effectively decreased due to its removal. The efficacy of carbon dioxide ( $CO_2$ ) adsorption through the utilization of potassium carbonate ( $K_2CO_3$ ) is contingent upon a multitude of variables, encompassing temperature, pressure, concentration of the  $K_2CO_3$  solution, and duration of interaction between the gaseous and liquid phases. In general, the process of adsorption is enhanced by higher temperatures and lower pressures. Furthermore, an increased concentration of  $K_2CO_3$  within the solution has been shown to enhance the efficiency of  $CO_2$  capture, as reported in reference [12]. [13].

The incorporation of nanoparticles (NPs) in conjunction with potassium carbonate ( $K_2CO_3$ ) has been found to improve the efficacy of carbon capture processes. Nanoparticles (NPs) provide a multitude of benefits, such as enhancing surface area and catalytic effect, that can enhance the absorption capacity and kinetics of carbon dioxide ( $CO_2$ ) capture, as indicated by previous research [14]. The enhanced surface area of nanoparticles facilitates improved interaction between the absorbent and  $CO_2$  molecules, thereby promoting increased  $CO_2$  uptake. This has been reported in literature [11]. The utilization of specific nanoparticles (NPs) can potentially enhance the catalytic activity, thereby promoting the reaction between  $CO_2$  and  $K_2CO_3$ . This, in turn, can expedite the production of potassium bicarbonate and augment the overall efficiency of  $CO_2$  sequestration, as reported in references [15] and [10].

Furthermore, the utilization of nanoparticles (NPs) can aid in reducing mass transfer limitations through the promotion of  $CO_2$  diffusion into the absorbent solution. The inclusion of nanoparticles (NPs) within a  $K_2CO_3$  solution has been observed to have a positive impact on the solubility of  $CO_2$ , leading to a reduction in mass transfer resistance [14]. This, in turn, has been shown to improve absorption kinetics and overall efficiency. The primary benefit of utilizing nanoparticles in conjunction with potassium carbonate lies in their capacity to stabilize and impede the deterioration of the absorbent solution, as noted in reference [16]. The efficacy of  $CO_2$  capture process may be impacted by the deterioration of  $K_2CO_3$  because of ancillary reactions or contaminants present in the flue gas. The inclusion of nanoparticles (NPs) has the potential to impede the degradation reactions and increases the durability of the absorbent solution, thereby guaranteeing its sustained efficacy. It is crucial to acknowledge that the effective integration of nanoparticles (NPs) in carbon dioxide ( $CO_2$ ) capture procedures necessitates meticulous contemplation of several aspects, such as the suitable NPs' choice, their dispersion in the solution, and their congruity with  $K_2CO_3$  [17]. The selection of NPs ought to be predicated upon their adsorption characteristics, stability, and cost-efficiency. It is crucial to employ accurate methods of characterization and optimize the concentration of nanoparticles to achieve the intended improvements in the efficiency of carbon capture. This has been highlighted in previous research [4], [16].

Incorporating piperazine as an adjunct in carbon sequestration techniques involving potassium carbonate ( $K_2CO_3$ ) has the potential to yield substantial advantages and augment the efficacy of  $CO_2$  capture. The cyclic organic compound known as Piperazine can function as a promoter or activator in the process of  $CO_2$  absorption, thereby resulting in an enhanced performance of carbon capture, as reported in reference [18],[4],[19]. Piperazine functions as a reactive solvent, facilitating the reaction between carbon dioxide and potassium carbonate, ultimately leading to the production of potassium bicarbonate. The enhancement in the reaction rate facilitates the efficacy of  $CO_2$  assimilation, thereby enabling elevated  $CO_2$  sequestration rates and diminishing the duration of contact necessary for proficient capture [12]. Piperazine has been found to possess not only promotional effects on  $CO_2$  absorption but also the ability to alleviate the degradation of  $K_2CO_3$  resulting from side reactions or impurities present in the flue gas. [14]. The maintenance of stability is of utmost importance for the sustainable functioning and financial feasibility of the carbon capture mechanism over an extended period. Nevertheless, it is crucial to consider the possible obstacles linked to the utilization of piperazine [20][21]. An area of concern pertains to the possible instability and vapor pressure exhibited by piperazine, which may lead to its dissipation via evaporation while undergoing the capture procedure. It is recommended that appropriate control measures and system design be employed in order to mitigate any potential losses of piperazine and optimize its efficacy, as per source [6].

This project intends to promote an innovative and efficient carbon capture technology, by using potassium carbonate ( $K_2CO_3$ ), piperazine, and nanoparticles to create a novel carbon sequestration blend in a polytetrafluoroethylene (PTFE) hollow fiber membrane contactor (HFMC) and perform a parametric analysis to assess its performance. Gas and liquid flow rates,  $K_2CO_3$  concentration and temperature manipulation will dominate the study. By examining how the effect of these operational factors determine carbon capture efficiency.

Parametric analysis evaluates many performance metrics.  $CO_2$  absorption rate, removal efficiency, and solvent stability. The experimental results will be analyzed to determine the synergistic effects of  $K_2CO_3$ , piperazine, and nanoparticles and their sensitivity to temperature and flow rates. Parametric analysis can help identify optimum operating parameters that enhance carbon capture efficiency while balancing energy needs and system stability.

## 2. EXPERIMENTAL WORK

The process of absorbing carbon dioxide involves the utilization of a PTFE membrane module manufactured by Nanjing Junxin Environmental Technology Co., Ltd. for the purpose of  $CO_2$  sequestration using blend of potassium carbonate ( $K_2CO_3$ ), piperazine, and nanoparticles. The aim of this study is to conduct a parametric analysis on the performance of the mixture, with a specific focus on the manipulation of gas and liquid flow rates and temperature. Initially, a solution of 10% wt. concentration is prepared by dissolving potassium carbonate ( $K_2CO_3$ ) in distilled water. The solution is subjected to magnetic stirring at ambient temperature for a duration of 30 minutes to attain uniformity. The solution's pH was measured to be pH: 10. Nanofluids are produced by incorporating nanomaterials, such as titanium dioxide and silica nanoparticles, into the underlying fluid. The nanomaterials were homogeneously dispersed in the base fluid through a combination of magnetic stirring for a duration of 30 minutes, followed by sonication in a water bath sonicator for a duration of 60 minutes. This guarantees a homogeneous dispersion of the nanomaterials within the solution. Piperazine of 2% is also prepared for experimental purposes. Figure 1 depicts the experimental apparatus.

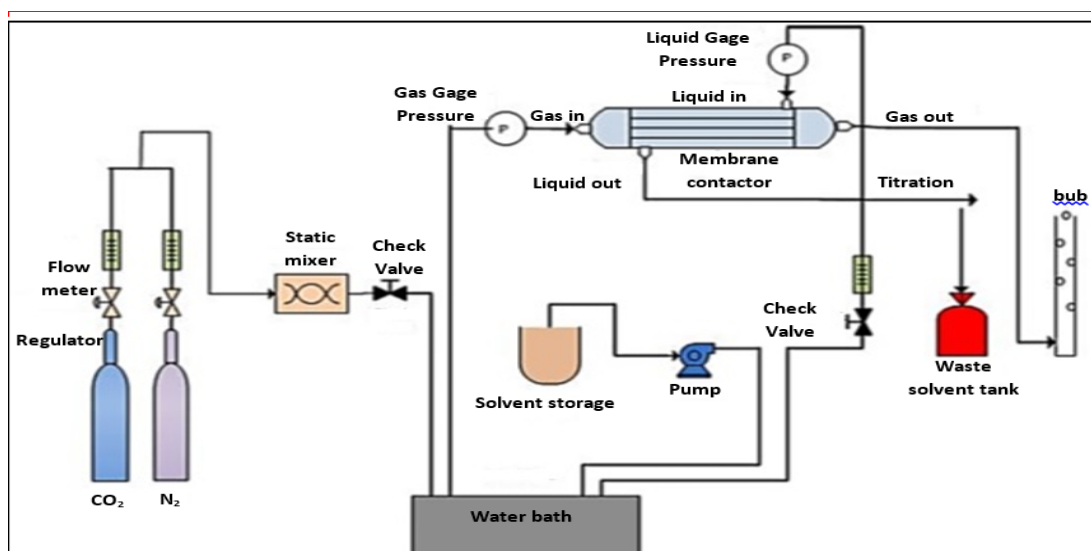


Fig 1a. Rig setup.

The process of absorbing carbon dioxide involves the utilization of a PTFE membrane module. The experimental setup comprises a module of a membrane contactor with hollow fibers, along with flow meters for both gas and liquid, pressure indicators, regulators, a static mixer for gases, a temperature controller, and a water bath. The transfer of absorbent from the solvent container to the internal lumen of the membrane module is facilitated by means of a peristaltic pump. A mixture of carbon dioxide and nitrogen gas is generated by a static mixer and subsequently passed through a water bath for temperature control, than it is directed towards the tube side of the membrane module. The coiled tube is supplied with an absorbent solvent which is then directed in a counter-current flow configuration towards the shell side of the membrane contactor module. The experimental assessments were carried out under a differential pressure of 0.2 atm between the gaseous and liquid phases along the investigation. We prevent the occurrence of bubbles within the mass transfer layer situated on the membrane surface, in order to uphold a consistently even mass transfer layer. After 15 minutes, the system attains its steady state. Following each testing cycle, the membrane module and pipes undergo a cleaning process utilizing distilled water, followed by drying with nitrogen gas to eliminate any remaining moisture. To mitigate membrane wetting and condensation effects, a valve is inserted into the liquid stream to impede the generation of gas bubbles. To avoid condensation, it is necessary to maintain a slightly higher pressure on the liquid side of the system compared to the gas side. Furthermore, the estimation of mass transfer and the amount of carbon dioxide assimilated from the surroundings is conducted through appropriate equations. The mixture liquid with  $K_2CO_3$ , incorporating piperazine (PZ), and the nanofluid with nanoparticles are prepared in following way:

- ❖ The initial step involves the preparation of the basic solution. To obtain a desired concentration, the necessary quantity of  $K_2CO_3$  is dissolved in distilled water at ambient temperature. The pH of the solution is controlled to verify if it falls within the specified range, if relevant.
- ❖ The preparation of the PZ solution uses PZ powder which is incorporated into the base fluid acquired in the first step.
- ❖ The suspension is mixed by magnetic stirrer for a duration of 10 minutes.
- ❖ To prepare the nanofluid, at the desired concentration of titanium dioxide or silica nanoparticles in the base fluid. The nanoparticles are incorporated into the base fluid under continuous stirring with a magnetic stirrer for a duration of 30 minutes to ensure a homogeneous dispersion. The nanofluid suspension is introduced in an ultrasonicator apparatus for a duration of 30 minutes. As cited by [66, 98], by this way the dispersion is stabilized and the aggregation nanoparticle is avoided.

### 3. ANALYSIS METHODOLOGY

To determine the percentage of carbon dioxide removal, we compare the quantity of carbon dioxide that has been eliminated to the inlet concentration of carbon dioxide. The carbon dioxide removal percentage can be computed using the subsequent formula.:

$$\text{Carbon Dioxide Removal \%} = \frac{(\text{Initial CO}_2 \text{ Concentration} - \text{Final CO}_2 \text{ Concentration})}{\text{Initial CO}_2 \text{ Concentration}} \times 100 \quad (1)$$

The methodological protocol elucidated above exemplifies the procedure for ascertaining the initial concentration of carbon dioxide and its subsequent sequestration via conduction employing  $\text{K}_2\text{CO}_3$ , piperazine, and a solution of nanofluid. Concentration measurements are conducted using analytical techniques such as gas chromatography or spectrophotometry. The discrepancy between the initial and final concentrations is quantified, and the proportion of carbon dioxide elimination is assessed utilizing Equation (1).

In order to explore the impact of variables such as the percentage of  $\text{K}_2\text{CO}_3$ , NPs,  $Q_L$ ,  $Q_g$ , and T on the process of carbon dioxide removal, we employ the Minitab software for sophisticated statistical analysis. The empirical observations are meticulously collected and organized in a systematic manner, while the requisite calculations of descriptive statistics are performed to elucidate the dataset's measures of central tendency and dispersion. Regression analysis, specifically employing multiple linear or polynomial regression techniques, is employed to evaluate the influence of various parameters on the process of carbon dioxide removal. The selection of a suitable model holds utmost importance in the process of determining the optimal regression model, wherein metrics such as R-squared, p-values, and ANOVA results play a pivotal role.

The parameter estimates derived from the regression analysis offer valuable insights into the intricate interplay between variables and the process of carbon dioxide removal. Minitab's optimization tools facilitate the determination of optimal parameter configurations that maximize the elimination of carbon dioxide, taking into account various constraints and objectives. The statistical analysis findings are duly interpreted, and a thorough examination is conducted to discern their implications for the process of carbon dioxide sequestration. A sensitivity analysis quantifies the resilience of the outcomes to variations in parameter values, thereby addressing potential limitations or ambiguities.

## 4. RESULTS AND DISCUSSION

### 4.1 The Effect of Liquid and Gas Flow Rates

The data that was observed indicates a distinct pattern where an increase in the rates of liquid flow rate ( $Q_L$ ) results in an increase in the efficiency of  $\text{CO}_2$  removal, as illustrated in Figures 2. The liquid volumetric flow rate varied from 53ml/min to 82 ml/min. It is shown that removal efficiency increased by 72%, 78%, 93%, 95% for ( $\text{K}_2\text{CO}_3$ ), ( $\text{K}_2\text{CO}_3/\text{PZ}$ ), ( $\text{K}_2\text{CO}_3/\text{PZ}/\text{SiO}_2$ ), and ( $\text{K}_2\text{CO}_3/\text{PZ}/\text{TiO}_2$ ) respectively. The mass transfer enhancement in the nanofluids caused is due to the grazing effect, Brownian motion and Micro convection. According to the grazing effect, the nanoparticles adsorbed the molecules of dissolved gas in a small film, and moving right through the concentration boundary layer, at last desorb the adsorbed molecules into the liquid bulk [22]. The presence of nanoparticles also can causes micro convection due to the nanoparticles Brownian motion; in fact, the micro convection can enhance the mass diffusion in the nanofluid. Because of the higher absorbing rate between  $\text{CO}_2$  and  $\text{K}_2\text{CO}_3$ ,  $\text{K}_2\text{CO}_3/\text{TiO}_2/\text{PZ}$  nanofluids outperformed  $\text{K}_2\text{CO}_3/\text{SiO}_2/\text{PZ}$  nanofluids in terms of  $\text{CO}_2$  absorption. Because  $\text{TiO}_2$  adsorbed more  $\text{CO}_2$ , the concentration gradient of  $\text{CO}_2$  increasing, and the absorption enhancement grew accordingly. It was shown that  $\text{K}_2\text{CO}_3/\text{PZ}/\text{TiO}_2$  nanofluids offered a greater rate of enhancement, Where efficiency has increased from 35% to 95%. Similarly slanted findings to those of this research were also reported by [39]. Conversely, the  $\text{CO}_2$  removal efficiency decreased from 86% to 63% when the gas volumetric flow rate was increased from 250 ml/min to 500 ml/min, as shown in fig.3

By increasing the gas flow rate concentration, CO<sub>2</sub> removal efficiency for all nanoparticles type reduces. The CO<sub>2</sub> residence time inside the fibers decreases and therefore lower amount of CO<sub>2</sub> can be absorbed through membrane into solvent [23].

The findings of this research are consistent with ref. [24][25][26]. Furthermore, the CO<sub>2</sub> removal efficiency for all nanoparticle types decreases as the gas flow rate increases. The increase of gas flow rate would accumulate the CO<sub>2</sub> Intensity. This phenomenon may results in a reduction in the efficacy of carbon dioxide removal. In situations where flow rates are elevated, the liquid contact time is so short on the shell side of the membrane contactor, to acheive substantial sequestration of CO<sub>2</sub> molecules, [27].

In order to ascertain the optimal range of flow rates, further investigation can be carried out through the utilization of experimental design methodologies like response surface methodology or factorial design. The present experiments investigates various flow rates for both the liquid and gas phases. Through a systematic manipulation of flow rates and the monitoring of CO<sub>2</sub> removal efficiency, it is possible to generate a response surface or contour plot that visually represents the relationship between flow rates and CO<sub>2</sub> capture efficiency. The present analysis conducts to the most favorable flow rate conditions, in our operating conditions, that can improve the efficiency of CO<sub>2</sub> removal [5],[11]. Furthermore, it is noteworthy to state that the inclusion of TiO<sub>2</sub> nanoparticles as additives resulted in a 43% increase in capture efficiency, whereas the incorporation of SiO<sub>2</sub> led to a 36% improvement. The incorporation of used additives has the potential to enhance the overall efficiency of the CO<sub>2</sub> capture procedure. When adding PZ to solution leads to increase CO<sub>2</sub> loading, the incorporation of piperazine results in a marginal increase in the capture efficiency across diverse liquid flow rates. According to the experimental results, the incorporation of piperazine results in a marginal increase of 2% in the capture efficiency across diverse gas and liquid flow rates. The aforementioned observations imply that the existence of piperazine results in a marginal enhancement in the efficacy of CO<sub>2</sub> sequestration. The utilization of piperazine as a solvent additive in CO<sub>2</sub> capture procedures is prevalent owing to its capacity to augment the absorption characteristics of the solvent. The facilitation of the reaction between carbon dioxide (CO<sub>2</sub>) and the solvent can lead to an enhancement of the capture efficiency [18].

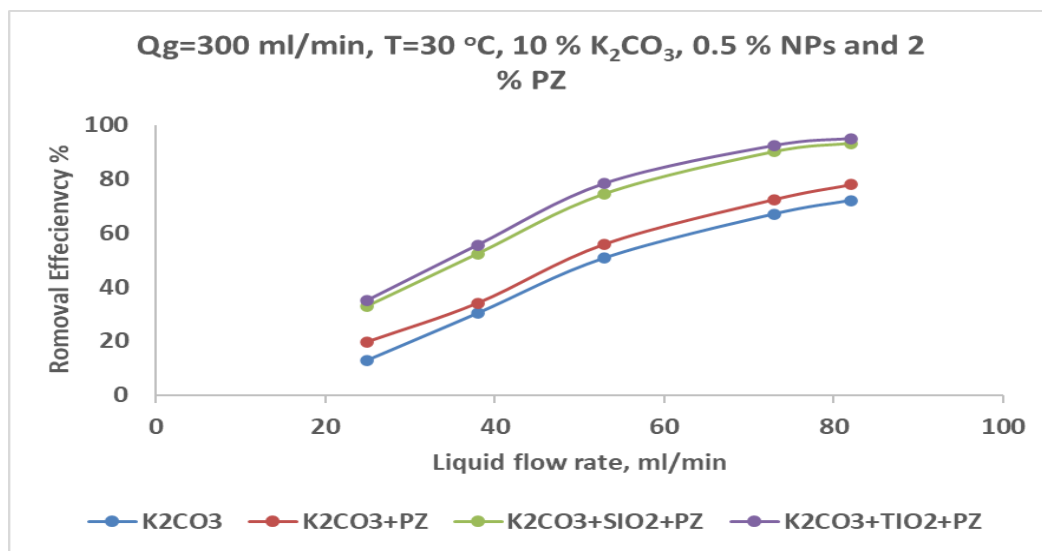


**Fig 2:** The impact of Liquid flow rate on CO<sub>2</sub> removal efficiency.

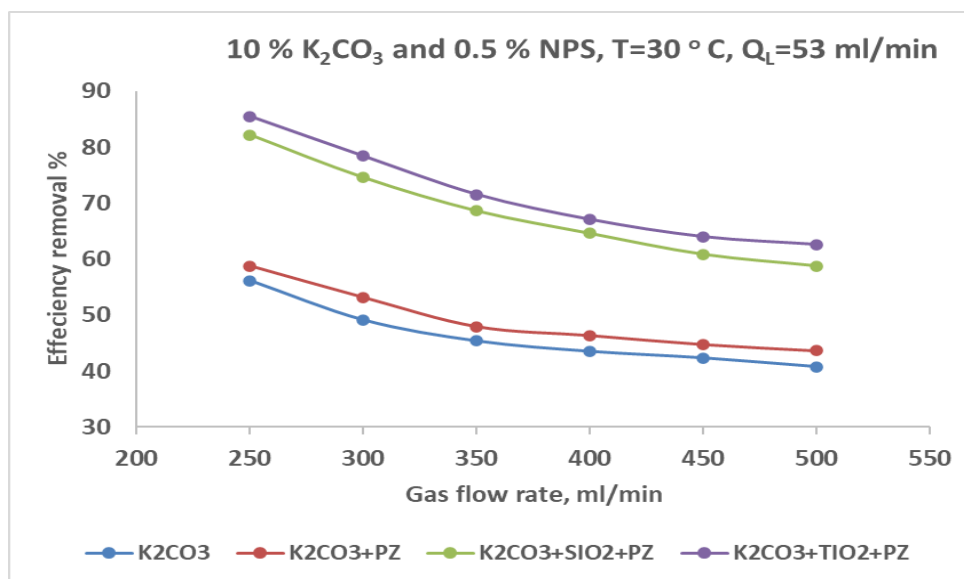


**Fig 3:** The impact of Gas flow rate on CO<sub>2</sub> removal efficiency.

#### 4.2 The Impact of K<sub>2</sub>CO<sub>3</sub> Concentration.

The findings depicted in Figure 4 indicate that there is a significant correlation between the percentage of K<sub>2</sub>CO<sub>3</sub> and the efficiency of CO<sub>2</sub> removal, whereby an increase in the former from 6.0% to 14.0%wt. K<sub>2</sub>CO<sub>3</sub>, results in a noteworthy improvement in the latter. The nanofluid volumetric flow rate and gas volumetric flow rate were fixed at 53 ml/min and 300 ml/min, respectively, the CO<sub>2</sub> removal efficiency increased from 51% to 92%. The CO<sub>2</sub> capture process experiences a notable enhancement as the concentration of K<sub>2</sub>CO<sub>3</sub> in the base fluid rises, leading to an increase in removal efficiency. This, in turn, facilitates a more efficient absorption of CO<sub>2</sub>. As a consequence, the efficiency of CO<sub>2</sub> removal is enhanced [8][28]. It is noteworthy that there exists a potential upper threshold for the concentration of K<sub>2</sub>CO<sub>3</sub>, beyond which any subsequent increments may not yield a substantial improvement in the efficacy of CO<sub>2</sub> sequestration. The observed phenomenon may be attributed to various factors, including limitations in CO<sub>2</sub> solubility or the possibility of side reactions that could arise at elevated concentrations.

Incorporating the impact of K<sub>2</sub>CO<sub>3</sub>, can facilitate an enhanced comprehension of the molecular interplay between CO<sub>2</sub> and K<sub>2</sub>CO<sub>3</sub>, and its consequent influence on the efficacy of CO<sub>2</sub> elimination. In conclusion, the data demonstrates a distinct indication that increasing the concentration of K<sub>2</sub>CO<sub>3</sub> in the base solution has a positive effect on the efficiency of CO<sub>2</sub> removal. The aforementioned phenomenon can be attributed to the increased availability of reactive sites for the absorption of carbon dioxide, which exhibits a direct correlation with the concentration of potassium carbonate (K<sub>2</sub>CO<sub>3</sub>). However, further investigation is required to determine the optimal K<sub>2</sub>CO<sub>3</sub> concentration that maximizes CO<sub>2</sub> capture, while considering practical limitations and system constraints. The augmentation of K<sub>2</sub>CO<sub>3</sub> concentration from 6% to 14% exerts a noteworthy influence on amplifying all the systems, namely K<sub>2</sub>CO<sub>3</sub> alone, in conjunction with PZ, SiO<sub>2</sub> NPs, and TiO<sub>2</sub> NPs, to the extent of reaching a high enhancement rate.

The augmentation of K<sub>2</sub>CO<sub>3</sub> concentration leads to an improvement in the solvent's ability to assimilate and interact with CO<sub>2</sub> molecules. As a consequence of this phenomenon, the elimination of CO<sub>2</sub> from the gaseous phase is enhanced, leading to an increase in the overall capture efficacy. The incorporation of additives, namely PZ (piperazine), SiO<sub>2</sub> NPs (silicon dioxide nanoparticles), and TiO<sub>2</sub> NPs (titanium dioxide nanoparticles), in conjunction with the augmented concentration of K<sub>2</sub>CO<sub>3</sub>, results in a heightened capture efficacy. these additives play a role in enhancing the mass transfer kinetics or the overall absorption characteristics of the solvent [12]. The observed increase in the CO<sub>2</sub> removal efficiency by twice time in the best conditions suggests that the system has a capacity to achieve a significantly higher level of performance in comparison to the baseline conditions.

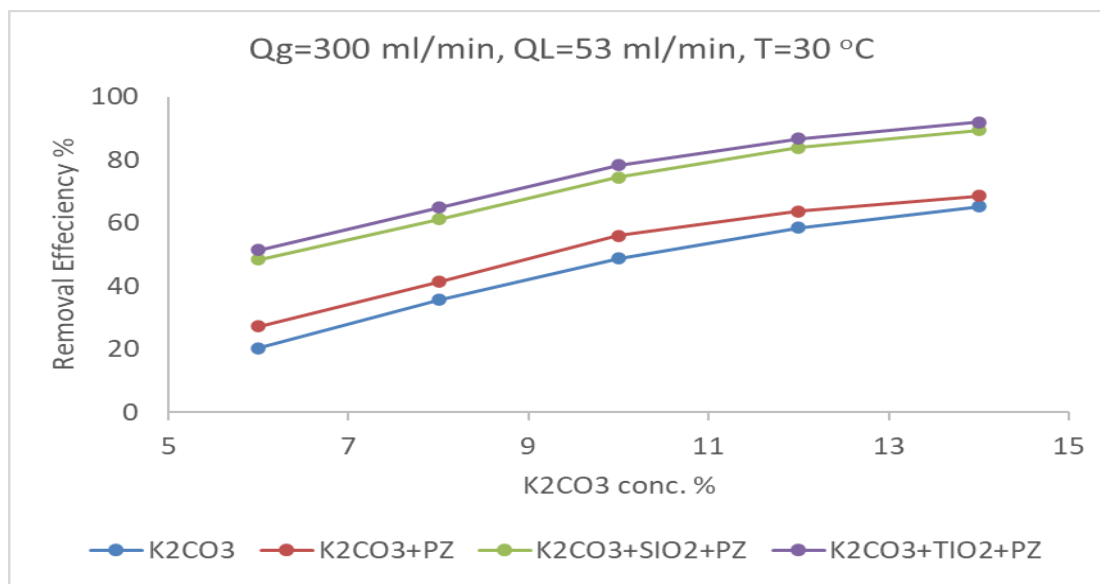


Fig. 4. The impact of  $K_2CO_3$  on removal efficiency.

### 4.3 The Impact of Nanomaterials

Figure 5 provides insights into the impact of silica ( $SiO_2$ ) and titanium oxide ( $TiO_2$ ) nanoparticles on the efficiency of carbon dioxide ( $CO_2$ ) removal. The investigated concentrations of  $TiO_2$  and  $SiO_2$  nanoparticles are 0.1 wt.%, 0.2 wt.%, 0.3 wt.%, 0.4 wt.%, 0.5 wt.%, 0.6 wt.%, and 0.7% wt with 2% piperazin (PZ). The volumetric flow rate of gas was 300 ml/min. The data suggests that the efficiency of  $CO_2$  removal peaked when at used nanoparticles concentration of 0.5%wt. and was shown to be optimal for  $CO_2$  absorption by these nanofluides as compared with other concentrations that studied and thereafter declined for both Nano fluids. At liquid flow rate of (53 ml/min) the removal efficiency was enhanced by 78%, 74% for  $K_2CO_3/PZ/TiO_2$ ,  $K_2CO_3/PZ/SiO_2$  respectively, the addition of  $TiO_2$  nanoparticles increased capture efficiency by 43%, while  $SiO_2$  enhanced it by 36%. The efficacy of nanoparticles depends on various factors, including their dimensions, surface properties, and interactions with the surrounding fluid [14].

it can be noticed that  $K_2CO_3/PZ/TiO_2$  nanofluid reveals better improved removal efficiency than  $K_2CO_3/PZ/SiO_2$  nanofluids, which reached to 78%. on the other hand, the performance of  $CO_2$

absorption decreased when nanoparticle concentration was higher than 0.5 Wt.%. Namely, there is an optimum concentration of nanoparticle for absorption of  $CO_2$  performance. An augmentation in the concentration of nanoparticles (NPs) exceeding 0.5% leads to a marginal decline in the capture efficiency. This phenomenon can be ascribed to the manifestation of membrane fouling, resulting in a decrease in the efficacy of capturing. Here, the above- mentioned phenomenon can be explained as follows nanoparticle amount and mutual interference increase with increasing nanoparticle concentration, that can improve the mass transfer according to the boundary mixing effect. The presence of the optimum concentration of nanofluids also observed by M.Darabi et al.[29]. In addition, an increase in the nanoparticles concentration may effect in the dispersion of the nanofluid and agglomeration of nanoparticles could take place. Therefore, the surface area of nanoparticles will be decreased. Furthermore, the nanoparticles movement will be hocked in the nanofluid by adjacent nanoparticles. Therefore, nanofluid absorption rate will decrease[26][30]. As mentioned earlier, the Brownian motion and shuttle effect of nanoparticles are two prominent mechanisms that explain the mass transfer enhancement in the nanofluides. Increasing the concentration of nanoparticle is expected to increasing both shuttle effect and micro convection that lead to improve mass transfer rate.



The previous works consistent the trend of this results [31][32][33]. When adding PZ to the absorbents leads to increase CO<sub>2</sub> absorption in solvents due to its molecular structure. It is an attractive carbon dioxide adsorbent, because two carbon dioxide molecules can be attached to a single piperazine molecule through two amine groups in the piperazine, thus improving absorption [34][35].

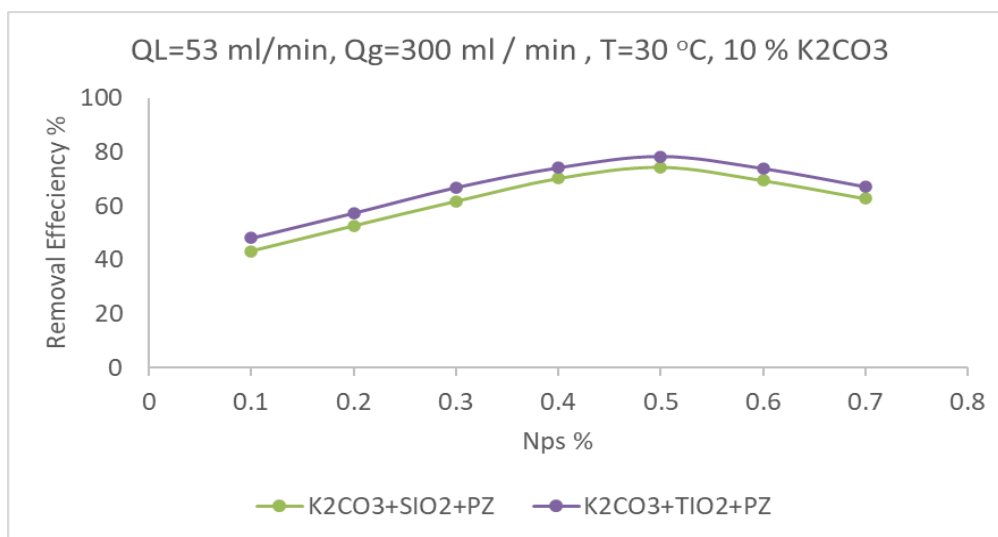


**Fig. 5:** The impact of nanoparticle conc. on removal efficiency.

The results of this investigation possess the potential to offer guidance for the progression of nanoparticle-based methodologies with enhanced efficacy. The examination of the available data suggests that the incorporation of isolated silica or titanium oxide nanoparticles at a concentration of 0.5% significantly impact the efficiency of CO<sub>2</sub> removal. Additional investigation is imperative to explore the potential of silica and titanium oxide nanoparticles and to optimize their concentration and properties with the aim of augmenting CO<sub>2</sub> capture [10].

#### 4.4 The Effect of Temperature

Figure 6 provides explicit information about the influence of temperature (T) on the efficiency of CO<sub>2</sub> removal in solvent strengthened by nanoparticles and PZ. at different temperatures of 20, 30, 40 and 50°C. The nanofluid volumetric flow rate was 53 ml/min, and the gas volumetric flow rate was 300 ml/min. The removal efficiency increased from 70% to 78% for K<sub>2</sub>CO<sub>3</sub>/PZ/TiO<sub>2</sub> nanofluid when the temperature increased from 20°C to 30°C. However, the CO<sub>2</sub> absorption performance is dropped when the temperature raised more than 30°C. The trends of the results are consistent with previous published works [23][24][36]. Temperature influences the kinetics of chemical reactions involved in CO<sub>2</sub> absorption by the base fluid or the interaction of CO<sub>2</sub> with adsorbent materials. Changes in temperature alter the rate of CO<sub>2</sub> sequestration and affect the equilibrium state of the sequestration mechanism and increase diffusivity of the species and the reaction rate constant according to the Arrhenius expression beside the thermodynamics Negative Gibbs free energy increases by temperature increasing [37, 38]. On the other hand, an increase in temperature can also cause a decrease in CO<sub>2</sub> solubility which reduces the effectiveness of CO<sub>2</sub> capture. Vapor fills the membrane pores, thus results in capillary condensation which can increase the membrane resistance which leads to a lower driving force for CO<sub>2</sub> absorption increase in absorbent evaporation and increase in CO<sub>2</sub> back-pressure which are not favorable for the absorption process [2],[24]. By increasing temperature, the Brownian movement and the aggregation of nanoparticles in absorption solutions may affected by temperature. This manner is further passionate in solution containing nanostructure due to the enhancement in the heat transfer caused by nanoparticles [3][24]. On the other hand, both mass and heat transfers have direct relationship with temperature. For nanofluids, higher suspension temperature will make stronger Brownian motion of suspended nanoparticles. Also, more intense microconvection inside the nanofluid, which further magnifies energy and mass transfer processes inside the nanofluid [39].

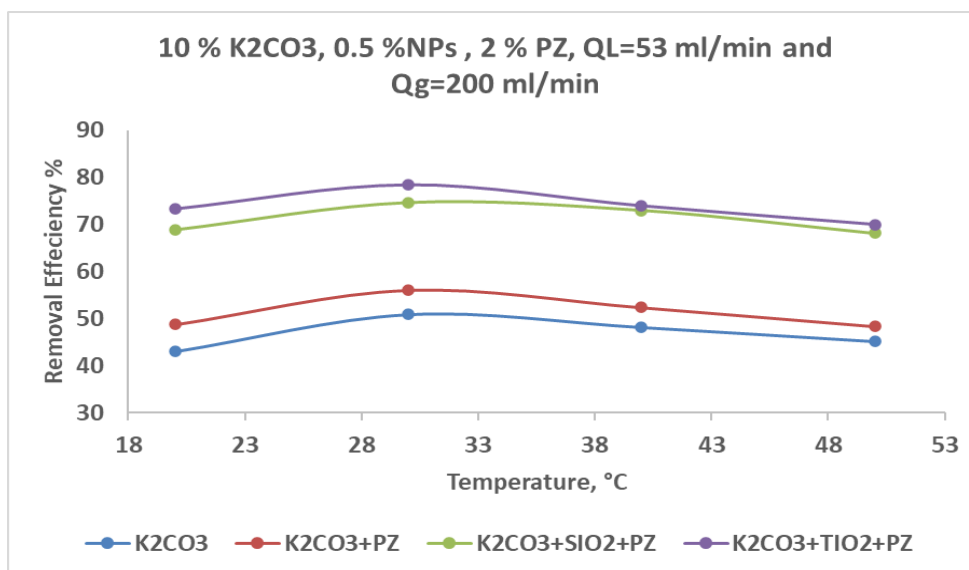


Fig. 6: The impact of Temp. on removal efficiency.

#### 4.5. Statistics Analysis

The design of experiments (DOE) is a powerful approach used to systematically plan, conduct, and analyze experiments. It allows researchers to efficiently investigate the effects of multiple factors on a response variable while controlling for potential confounding variables. By carefully selecting the levels of each factor and replicating the experiment, DOE enables the identification of significant factors and interactions, leading to a comprehensive understanding of the underlying relationships.

Once the experimental data is collected, statistical methods such as Analysis of Variance (ANOVA) and regression are commonly employed for data analysis. ANOVA assesses the significance of differences among means of multiple groups and helps determine whether there are statistically significant effects of individual factors or their interactions on the response variable. It quantifies the variability between and within groups to make inference about the overall differences. Regression analysis, on the other hand, explores the relationship between a dependent variable (response) and one or more independent variables (predictors). It fits a mathematical model to the data and estimates the coefficients of the predictors, indicating the magnitude and direction of their influence on the response variable. Regression analysis is particularly useful for understanding the impact of continuous variables on the response and predicting outcomes based on the model. The regression table is an essential output of the regression analysis. It presents the estimated coefficients, their standard errors, t-values, p-values, and other statistical measures. The coefficients represent the expected change in the response variable associated with a one-unit change in each predictor while holding other factors constant. The standard errors provide a measure of the uncertainty in the coefficient estimates, and the t-values and p-values indicate the significance of each predictor. By functionalizing the regression table, researchers can gain valuable insights into the strength and significance of the relationships between the predictors and the response variable. It allows for a clear interpretation of the coefficients and helps identify which factors have a significant impact on the response. This functionalization also aids in making data-driven decisions and formulating effective strategies based on the study's results.

Table 1 presents the results of a statistical analysis that explores the relationship between various factors (T, Q<sub>g</sub>, Q<sub>L</sub>, K<sub>2</sub>CO<sub>3</sub> %, PZ%, SiO<sub>2</sub> %, TiO<sub>2</sub> %) and CO<sub>2</sub> removal efficiency. The coefficients (Coef) in the table represent the estimated values of the regression model for each factor, indicating the expected change in CO<sub>2</sub> removal efficiency with a one-unit change in the corresponding factor while keeping other variables constant. The standard error of the coefficient estimates (SE Coef) provides a measure of uncertainty or variability associated with the estimated coefficients. The t-value measures the significance of each coefficient, with larger absolute t-values indicating stronger evidence against the null hypothesis of a zero coefficient. The p-value represents the probability of observing a t-value as extreme as calculated, assuming the null hypothesis is true. Lower p-values, typically below 0.05, indicate stronger evidence against the null hypothesis. The Variance Inflation Factor (VIF) assesses

multicollinearity between predictors, with values close to 1 indicating low multicollinearity. The constant term in the analysis represents the expected CO<sub>2</sub> removal efficiency when all other predictors are zero, which in this case is 74.19. The individual predictors (T, Q<sub>g</sub>, Q<sub>L</sub>, K<sub>2</sub>CO<sub>3</sub>%, PZ%, SiO<sub>2</sub>%, TiO<sub>2</sub>%) are examined in relation to CO<sub>2</sub> removal efficiency, and their coefficients indicate the expected change in CO<sub>2</sub> removal efficiency with a one-unit change in each factor. The associated p-values provide insights into the significance of each factor, where p-values less than 0.05 generally indicate a statistically significant relationship. Based on the provided information, it appears that Q<sub>g</sub>, Q<sub>L</sub>, K<sub>2</sub>CO<sub>3</sub>%, PZ%, SiO<sub>2</sub>%, and TiO<sub>2</sub>% have statistically significant effects on CO<sub>2</sub> removal efficiency. The non-zero coefficients associated with these factors suggest they have a meaningful impact on the response variable.

- Based on the provided information, it appears that Q<sub>g</sub>, Q<sub>L</sub>, K<sub>2</sub>CO<sub>3</sub> %, PZ%, SiO<sub>2</sub> %, and TiO<sub>2</sub> % have statistically significant effects on CO<sub>2</sub> removal efficiency. The coefficients associated with these factors are non-zero, suggesting they have a meaningful impact on the response variable.

Overall, this analysis provides insights into the relationships between the examined factors and CO<sub>2</sub> removal efficiency. However, it's important to note that additional context and further analysis would be required to fully understand the significance and practical implications of these findings in the specific research context.

**Table 1: coded coefficient analysis.**

Term	Coef	SE Coef	T-Value	P-Value	VIF
Constant	74.19	1.73	42.86	0.000	
T	-0.34	1.61	-0.21	0.836	1.01
Q <sub>g</sub>	29.74	1.55	19.14	0.000	1.00
Q <sub>L</sub>	-3.172	0.917	-3.46	0.001	1.01
K <sub>2</sub> CO <sub>3</sub> %	21.26	1.63	13.01	0.000	1.00
PZ%	2.144	0.792	2.71	0.008	1.48
SiO <sub>2</sub> %	12.69	1.04	12.17	0.000	1.55
TiO <sub>2</sub> %	14.99	1.04	14.38	0.000	1.55

Table 2 provides a comprehensive analysis of variance (ANOVA) for the regression model employed to examine the relationship between the predictors (T, Q<sub>g</sub>, Q<sub>L</sub>, K<sub>2</sub>CO<sub>3</sub> %, PZ%, SiO<sub>2</sub> %, TiO<sub>2</sub> %) and CO<sub>2</sub> removal efficiency. The table highlights key aspects of the analysis: the sources of variation including the Model, Linear predictors, Lack-of-Fit, and Pure Error; the associated degrees of freedom (DF); the Adjusted Sum of Squares (Adj SS) and Adjusted Mean Square (Adj MS) reflecting the variance adjusted for DF; the F-Value indicating the significance of predictor-response relationship; and the corresponding p-values. Interpretation of the results reveals that the overall model, encompassing all predictors, demonstrates a highly significant connection with CO<sub>2</sub> removal efficiency, substantiated by a substantial F-value of 140.09 and a minuscule p-value of 0.000. Among the individual predictors, except for T (p-value = 0.836), each exhibits a statistically significant association with CO<sub>2</sub> removal efficiency, evident from their low p-values. The Error term represents unexplained variation, while the noteworthy significance of the Lack-of-Fit term implies the potential presence of nonlinear relationships or unaccounted factors influencing CO<sub>2</sub> removal efficiency beyond the linear model. The Total variation represents the raw sum of squares for the response variable without adjustments.

Overall, the ANOVA results indicate that the model, including the predictors Q<sub>g</sub>, Q<sub>L</sub>, K<sub>2</sub>CO<sub>3</sub> %, PZ%, SiO<sub>2</sub> %, and TiO<sub>2</sub> %, has a significant relationship with CO<sub>2</sub> removal efficiency. However, it's important to note that the lack-of-fit term suggests that the linear model might not fully capture all the variability in the data, indicating the need for further analysis or consideration of additional factors.

Table 2: ANOVA table.

Source	DF	Adj SS	Adj MS	F-Value	P-Value
Model	7	26199.2	3742.74	140.09	0.000
Linear	7	26199.2	3742.74	140.09	0.000
T	1	1.2	1.16	0.04	0.836
Qg	1	9788.8	9788.76	366.38	0.000
QL	1	319.5	319.53	11.96	0.001
K <sub>2</sub> CO <sub>3</sub> %	1	4520.0	4520.03	169.18	0.000
PZ%	1	195.7	195.72	7.33	0.008
SiO <sub>2</sub> %	1	3959.0	3959.01	148.18	0.000
TiO <sub>2</sub> %	1	5524.9	5524.85	206.79	0.000
Error	86	2297.7	26.72		
Lack-of-Fit	76	2294.7	30.19	100.76	0.000
Pure Error	10	3.0	0.30		
Total	93	28496.9			

The regression equation provided is:

$$\text{Removal efficiency \%} = -56.41 - 0.022T + 1.0434Qg - 0.02115QL + 531.5K_2CO_3\% + 214.4PZ\% + 3625SiO_2\% + 4282TiO_2\% \quad (2)$$

Here's an interpretation of the statistical measures associated with the regression model:

- S: The estimated standard deviation of the residuals is 5.16891. It represents the average distance between the observed data points and the predicted values from the regression equation.
- R-squared (R-sq): R-squared is a measure of the proportion of the total variability in the response variable that can be explained by the regression model. In this case, the R-squared value of 91.94% indicates that approximately 91.94% of the variation in CO<sub>2</sub> removal efficiency can be explained by the predictors included in the model.
- R-squared adjusted (R-sq(adj)): The adjusted R-squared takes into account the number of predictors and the degrees of freedom in the model. It penalizes the inclusion of additional predictors that do not significantly contribute to the model's fit. The R-squared adjusted value of 91.28% suggests that the predictors in the model explain a substantial amount of the variability in CO<sub>2</sub> removal efficiency.
- R-squared predicted (R-sq(pred)): The R-squared predicted provides an estimate of how well the regression model can predict future observations. The R-squared predicted value of 90.63% indicates that the current model has a good predictive capability for CO<sub>2</sub> removal efficiency.

Overall, the regression model shows a high level of goodness-of-fit, as indicated by the high R-squared and R-squared adjusted values. It suggests that the predictors (T, Q<sub>g</sub>, Q<sub>L</sub>, K<sub>2</sub>CO<sub>3</sub>%, PZ%, SiO<sub>2</sub>%, TiO<sub>2</sub>%) included in the model collectively explain a significant portion of the variation in CO<sub>2</sub> removal efficiency. The R-squared predicted value suggests that the model can reasonably predict the CO<sub>2</sub> removal efficiency for new or future data points.

To create a Pareto chart for the given expression of the removal efficiency, we need to consider the magnitudes of the coefficients associated with each variable. The Pareto chart will help us identify the most significant factors contributing to the removal efficiency.

Here is the breakdown of the variables and their coefficients:

- T: Temperature coefficient = -0.022
- Q<sub>g</sub>: Gas flow rate coefficient = 1.0434
- Q<sub>L</sub>: Liquid flow rate coefficient = -0.02115
- K<sub>2</sub>CO<sub>3</sub> %: K<sub>2</sub>CO<sub>3</sub> percentage coefficient = 531.5
- PZ %: PZ percentage coefficient = 214.4
- SiO<sub>2</sub> %: Silica percentage coefficient = 3625
- TiO<sub>2</sub> %: Titanium oxide percentage coefficient = 4282

Using these coefficients, we can construct the Pareto chart (Fig 7) by arranging the variables in descending order of their absolute values. The Pareto chart will have bars representing the absolute values of the coefficients for each variable. The tallest bar will represent the variable with the highest absolute coefficient value, indicating its significant influence on the removal efficiency. The bars will be arranged from left to right in decreasing order of their heights.

The cumulative percentage line in the chart will show the cumulative contribution of the variables to the total variability explained by the expression. It will start at zero and gradually increase as each variable is added, eventually reaching 100% at the end. By examining the Pareto chart, you can easily identify the variables with the largest bars, indicating their significant impact on the removal efficiency. Additionally, the cumulative percentage line will help you understand how much of the total variability in the removal efficiency is explained by including a certain number of variables.

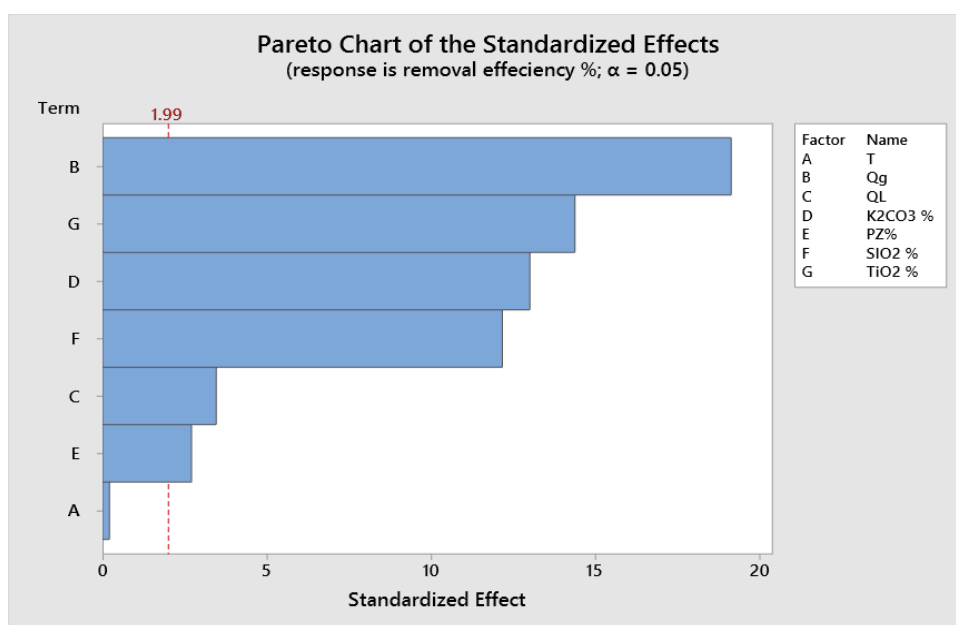
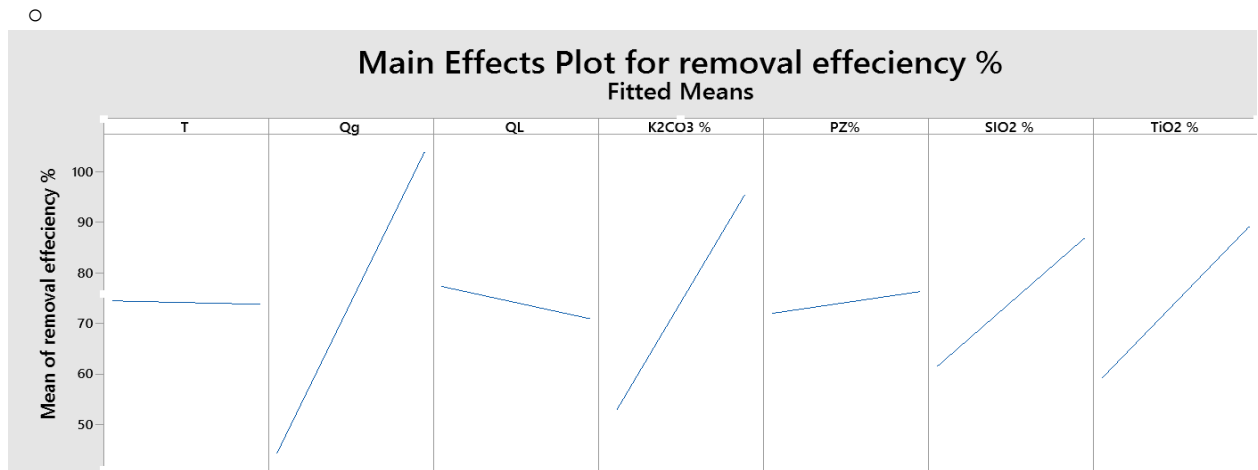


Fig. 7 Pareto chart of present work.

#### 4.6 Optimization Analysis

We can assess the sensitivity of each parameter by examining their respective coefficients as shown in Fig 8:

- T (Temperature): The coefficient is -0.022. A negative coefficient indicates that as temperature increases, removal efficiency decreases. The magnitude of -0.022 suggests that temperature has a relatively small impact on removal efficiency compared to other parameters.
- $Q_g$  (Gas flow rate): The coefficient is 1.0434. A positive coefficient indicates that as gas flow rate increases, removal efficiency increases. The magnitude of 1.0434 suggests that  $Q_g$  has a moderate impact on removal efficiency.
- $Q_L$  (Liquid flow rate): The coefficient is -0.02115. A negative coefficient indicates that as liquid flow rate increases, removal efficiency decreases. The magnitude of -0.02115 suggests that  $Q_L$  has a relatively small impact on removal efficiency compared to other parameters.
- $K_2CO_3$  % ( $K_2CO_3$  percentage): The coefficient is 531.5. A positive coefficient indicates that as the percentage of  $K_2CO_3$  increases, removal efficiency increases. The magnitude of 531.5 suggests that  $K_2CO_3$  % has a significant impact on removal efficiency.
- PZ% (PZ percentage): The coefficient is 214.4. A positive coefficient indicates that as the percentage of PZ increases, removal efficiency increases. The magnitude of 214.4 suggests that PZ% has a significant impact on removal efficiency.
- $SiO_2$ % (Silica percentage): The coefficient is 3625. A positive coefficient indicates that as the percentage of silica increases, removal efficiency increases. The magnitude of 3625 suggests that  $SiO_2$ % has a substantial impact on removal efficiency.
- $TiO_2$ % (Titanium oxide percentage): The coefficient is 4282. A positive coefficient indicates that as the percentage of titanium oxide increases, removal efficiency increases. The magnitude of 4282 suggests that  $TiO_2$ % has a substantial impact on removal efficiency.



**Fig 8:** Factorial analysis for parameters sensitivity finding.

The objective with regards to the removal efficiency, as per the provided data, is to attain a maximal value. The absence of specified lower and upper bounds implies the lack of predetermined thresholds for the removal efficiency. The absence of the target value is also not specified. The removal efficiency has been assigned a weight of 1, signifying its paramount significance in the analysis.

The proposed solution encompasses a range of independent variable configurations, namely T,  $Q_g$ ,  $Q_L$ ,  $K_2CO_3$  %, PZ%,  $SiO_2$  %, and  $TiO_2$  %. The corresponding removal efficiency is predicted through the application of a regression model.

Regarding the particular resolution:

- The temperature was set to 30 °C.

- The gas flow rate ( $Q_g$ ) was established at a value of 200.
- The liquid flow rate, denoted as  $Q_L$ , was established at a value of 82.
- The  $K_2CO_3$  percentage was established at 0.14.
- The PZ percentage is established at 2%.
- The silica percentage, denoted as  $SiO_2\%$ , has been established at 0.7%.
- The percentage of titanium oxide ( $TiO_2\%$ ) has been established at 0.7%.

The removal efficiency anticipated from these parameters is 158.51, accompanied by a standard error of 3.79. The predicted removal efficiency is associated with a 95% confidence interval (CI) of (150.98; 166.05), while the 95% prediction interval (PI) is estimated to be (145.77; 171.26).

## CONCLUSIONS

Based on the experimental results obtained in this investigation, it can be deduced that there is a direct correlation between the efficacy of carbon dioxide ( $CO_2$ ) removal and the velocity of liquid flow ( $Q_L$ ), while an inverse relationship is observed between the efficiency of  $CO_2$  removal and the velocity of gas flow ( $Q_g$ ). This observation implies the presence of a spectrum of flow rates that may enhance the efficiency of  $CO_2$  sequestration. The effectiveness of carbon dioxide ( $CO_2$ ) removal is directly influenced by the concentration of potassium carbonate ( $K_2CO_3$ ) in the liquid, wherein higher amounts of  $K_2CO_3$  lead to improved operational efficiency. The observed effectiveness of carbon dioxide ( $CO_2$ ) elimination was found to be significantly impacted by the inclusion of titanium dioxide ( $TiO_2$ ) nanoparticles at a concentration of 0.5% and 2%PZ as opposed to silica ( $SiO_2$ ) nanoparticles. The inquiry further determined that the optimal temperature for  $CO_2$  removal was observed to be  $30^\circ C$ . The statistical analysis reveals that the variables  $Q_g$ ,  $Q_L$ ,  $K_2CO_3\%$ , PZ%,  $SiO_2\%$ , and  $TiO_2\%$  manifest noteworthy influences on the efficacy of  $CO_2$  elimination. The ANOVA analysis has unveiled a chemically significant correlation between the efficiency of carbon dioxide ( $CO_2$ ) elimination and the comprehensive model encompassing all predictors. Nevertheless, the existence of a deficiency-of-match constituent in the linear model implies the potential occurrence of unaccounted variability, thereby indicating the plausible impact of additional factors that have not been taken into account in the present model. Henceforth, it may be imperative to conduct additional scrutiny or incorporate supplementary variables to enhance comprehension and apprehension of the comprehensive panorama pertaining to  $CO_2$  elimination efficacy. In order to maximize the efficiency of  $CO_2$  elimination, it is imperative to optimize the flow rates, concentration of  $K_2CO_3$ , and characteristics of the nanoparticles. The objective of the analysis is to optimize the removal efficiency, as indicated by the weight assigned to this parameter. The lack of well-defined lower and upper thresholds, along with an absence of a specified desired value for the elimination efficacy, was observed. The proposed methodology involves the determination of exact numerical values for the independent variables, specifically temperature (T) set at  $30^\circ C$ , gas flow rate ( $Q_g$ ) maintained at 250, liquid flow rate ( $Q_L$ ) set at 82,  $K_2CO_3\%$  at 0.14, PZ% at 2%,  $SiO_2\%$  at 0.7%, and  $TiO_2\%$  at 0.7%.

## REFERENCES

- [1] M. Arishi, T. E. Akinola, and M. Wang, "Technical analysis of post-combustion carbon capture using  $K_2CO_3$  for large-scale power plants through simulation," *SSRN Electron. J.*, no. October, 2022, doi: 10.2139/ssrn.4282880.
- [2] I. Ham-Liu, J. A. Mendoza-Nieto, and H. Pfeiffer, "CO<sub>2</sub> chemisorption enhancement produced by  $K_2CO_3$ - and  $Na_2CO_3$ -addition on  $Li_2CuO_2$ ," *J. CO<sub>2</sub> Util.*, vol. 23, no. November 2017, pp. 143–151, 2018, doi: 10.1016/j.jcou.2017.11.009.
- [3] M. D. G. de Luna, A. S. Sioson, A. E. S. Choi, R. R. M. Abarca, Y. H. Huang, and M. C. Lu, "Operating pH influences homogeneous calcium carbonate granulation in the frame of CO<sub>2</sub> capture," *J. Clean. Prod.*, vol. 272, p. 122325, 2020, doi: 10.1016/j.jclepro.2020.122325.
- [4] H. Abdolahi-Mansoorkhani and S. Seddighi, "CO<sub>2</sub> capture by modified hollow fiber membrane contactor: Numerical study on membrane structure and membrane wettability," *Fuel Process. Technol.*, vol. 209, no. May, 2020, doi: 10.1016/j.fuproc.2020.106530.
- [5] Z. Pang, S. Jiang, C. Zhu, Y. Ma, and T. Fu, "Mass transfer of chemical absorption of CO<sub>2</sub> in a serpentine minichannel," *Chem. Eng. J.*, vol. 414, no. February, p. 128791, 2021, doi: 10.1016/j.cej.2021.128791.
- [6] J. Liu, Carbon capture using nanoporous adsorbents. INC, 2020. doi: 10.1016/b978-0-12-818487-5.00008-x.
- [7] V. Sang Sefidi and P. Luis, "Advanced Amino Acid-Based Technologies for CO<sub>2</sub> Capture: A Review," *Ind. Eng. Chem. Res.*, vol. 58, no. 44, pp. 20181–20194, 2019, doi: 10.1021/acs.iecr.9b01793.
- [8] J. Xie, L. Zhang, D. Fu, and H. Zhu, "CO<sub>2</sub> capture process and corrosion of carbon steel in [Bmim][Lys]- $K_2CO_3$  aqueous solutions," *Int. J. Electrochem. Sci.*, vol. 14, no. 1, pp. 634–650, 2019, doi: 10.20964/2019.01.57.

- [9] B. Sarici, S. Karatas, and E. Altintig, "Removal of Methylene blue from aqueous solution with activated carbon produced from hazelnut shells by K<sub>2</sub>CO<sub>3</sub> activation," *Desalin. Water Treat.*, vol. 254, pp. 287–301, 2022, doi: 10.5004/dwt.2022.28353.
- [10] J. Charoenchaipet, P. Piumsomboon, and B. Chalermstinsuwan, "Development of CO<sub>2</sub> capture capacity by using impregnation method in base condition for K<sub>2</sub>CO<sub>3</sub>/Al<sub>2</sub>O<sub>3</sub>," *Energy Reports*, vol. 6, pp. 25–31, 2020, doi: 10.1016/j.egy.2019.11.037.
- [11] L. Yue et al., CO<sub>2</sub> adsorption at nitrogen-doped carbons prepared by K<sub>2</sub>CO<sub>3</sub> activation of urea-modified coconut shell, vol. 511. 2018. doi: 10.1016/j.jcis.2017.09.040.
- [12] T. Moore, M. Biviano, K. A. Mumford, R. R. Dagastine, G. W. Stevens, and P. A. Webley, "Solvent Impregnated Polymers for Carbon Capture," *Ind. Eng. Chem. Res.*, vol. 58, no. 16, pp. 6626–6634, 2019, doi: 10.1021/acs.iecr.8b05603.
- [13] U. Kamran and S. J. Park, "Chemically modified carbonaceous adsorbents for enhanced CO<sub>2</sub> capture: A review," *J. Clean. Prod.*, vol. 290, p. 125776, 2021, doi: 10.1016/j.jclepro.2020.125776.
- [14] Y. Li, L. Wang, Z. Tan, Z. Zhang, and X. Hu, "Experimental studies on carbon dioxide absorption using potassium carbonate solutions with amino acid salts," *Sep. Purif. Technol.*, vol. 219, pp. 47–54, 2019, doi: 10.1016/j.seppur.2019.03.010.
- [15] I. Yanase, S. Konno, and H. Kobayashi, "Reversible CO<sub>2</sub> capture by ZnO slurry leading to formation of fine ZnO particles," *Adv. Powder Technol.*, vol. 29, no. 5, pp. 1239–1245, 2018, doi: 10.1016/j.apt.2018.02.016.
- [16] S. Seo, B. Lages, and M. Kim, "Catalytic CO<sub>2</sub> absorption in an amine solvent using nickel nanoparticles for post-combustion carbon capture," *J. CO<sub>2</sub> Util.*, vol. 36, no. October 2019, pp. 244–252, 2020, doi: 10.1016/j.jcou.2019.11.011.
- [17] M. E. Russo, P. Bareschino, F. Pepe, A. Marzocchella, and P. Salatino, "Modelling of enzymatic reactive CO<sub>2</sub> absorption," *Chem. Eng. Trans.*, vol. 69, pp. 457–462, 2018, doi: 10.3303/CET1869077.
- [18] B. Zhao, T. Fang, W. Qian, J. Liu, and Y. Su, "Process simulation, optimization and assessment of post-combustion carbon dioxide capture with piperazine-activated blended absorbents," *J. Clean. Prod.*, vol. 282, no. xxxx, p. 124502, 2021, doi: 10.1016/j.jclepro.2020.124502.
- [19] A. D. Wiheeb, S. W. Shakir, M. A. Ahmed, and E. A. Rajab, "Experimental investigation of carbon dioxide capturing into aqueous carbonate solution promoted by alkanolamine in a packed absorber," *1st Int. Sci. Conf. Eng. Sci. - 3rd Sci. Conf. Eng. Sci. ISCES 2018 - Proc.*, vol. 2018-January, pp. 152–156, 2018, doi: 10.1109/ISCES.2018.8340545.
- [20] S. Scheiter, G. R. Moncrieff, M. Pfeiffer, and S. I. Higgins, "Interactive comment on 'African biomes are most sensitive to changes in CO<sub>2</sub> under recent and near-future CO<sub>2</sub> conditions,'" *Biogeosciences*, pp. 1147–1167, 2020.
- [21] P. Librandi, P. Nielsen, G. Costa, R. Snellings, M. Quaghebeur, and R. Baciocchi, "Mechanical and environmental properties of carbonated steel slag compacts as a function of mineralogy and CO<sub>2</sub> uptake," *J. CO<sub>2</sub> Util.*, vol. 33, no. May, pp. 201–214, 2019, doi: 10.1016/j.jcou.2019.05.028.
- [22] R. L. Kars, R. J. B. 1, and A. A. H. Drinkenburg, 'The Sorption of Propane in Slurries of Active Carbon ;n Water', vol. 17, pp. 201–210, 1979.
- [23] A. Golkhar, P. Keshavarz, and D. Mowla, 'Investigation of CO<sub>2</sub> removal by silica and CNT nanofluids in microporous hollow fiber membrane contactors', *J. Memb. Sci.*, vol. 433, pp. 17–24, 2013, doi: 10.1016/j.memsci.2013.01.022.
- [24] H. Mohammaddoost, A. Azari, M. Ansarpour, and S. Osfour, 'Experimental investigation of CO<sub>2</sub> removal from N<sub>2</sub> by metal oxide nano fluids in a hollow fiber membrane contactor', *International Journal of Greenhouse Gas Control*, vol. 69, no. December 2017. Elsevier, pp. 60–71, 2018, doi: 10.1016/j.ijggc.2017.12.012.
- [25] Z. Z. Yifu Li, Li'ao Wang, 'Carbon dioxide absorption from biogas by amino acid salt promoted potassium carbonate solutions in a hollow fiber membrane contactor : A numerical study', 2018, doi: 10.1021/acs.energyfuels.7b03616.
- [26] A. Peyravi, P. Keshavarz, and D. Mowla, 'Experimental investigation on the absorption enhancement of CO<sub>2</sub> by various nanofluids in hollow fiber membrane contactors', 2015, doi: 10.1021/acs.energyfuels.5b01956.
- [27] W. Kim, H. U. Kang, and K. Jung, 'Separation Science and Technology Synthesis of Silica Nanofluid and Application to CO<sub>2</sub> Absorption', *Separation science Technol.*, no. July 2013, pp. 37–41, 2013, doi: 10.1080/01496390802063804.
- [28] Q. Li, Y. Wang, S. An, and L. Wang, 'Kinetics of CO<sub>2</sub> Absorption in Concentrated K<sub>2</sub>CO<sub>3</sub> / PZ Mixture by using a Wetted-Wall Column Gas-liquid', 2016, doi: 10.1021/acs.energyfuels.6b00793.
- [29] HAMID, M., Jam, F.A., Mehmood, S. (2019). Psychological Empowerment and Employee Attitudes: Mediating Role of Intrinsic Motivation. *International Journal of Business and Economic Affairs*, 4(6), 300-314.
- [30] M. Darabi, M. Rahimi, and A. M. Dehkordi, 'Gas Absorption Enhancement in Hollow Fiber Membrane Contactors using', *Chem. Eng. Process. Process Intensif.*, 2017, doi: 10.1016/j.cep.2017.05.007.
- [31] B. Rahmatmand, P. Keshavarz, and S. Ayatollahi, 'Study of Absorption Enhancement of CO<sub>2</sub> by SiO<sub>2</sub>, Al<sub>2</sub>O<sub>3</sub>, CNT, and Fe<sub>3</sub>O<sub>4</sub> Nanoparticles in Water and Amine Solutions', 2016, doi: 10.1021/acs.jced.5b00442.
- [32] M. Rezakazemi, M. Darabi, E. Soroush, and M. Mesbah, 'CO<sub>2</sub> absorption enhancement by water-based nanofluids of CNT and SiO<sub>2</sub> using hollow-fiber membrane contactor', *Sep. Purif. Technol.*, vol. 210, pp. 920–926, 2019, doi: 10.1016/j.seppur.2018.09.005.
- [33] J. W. Lee, I. T. Pineda, J. H. Lee, and Y. T. Kang, 'Combined CO<sub>2</sub> absorption / regeneration performance enhancement by using nanoabsorbents', *Appl. Energy*, vol. 178, pp. 164–176, 2016, doi: 10.1016/j.apenergy.2016.06.048.
- [34] Z. Zhang, J. Cai, F. Chen, H. Li, W. Zhang, and W. Qi, 'Progress in enhancement of CO<sub>2</sub> absorption by nanofluids: A mini review of mechanisms and current status', *Renew. Energy*, vol. 118, pp. 527–535, 2018, doi: 10.1016/j.renene.2017.11.031.
- [35] W. Conway, D. Fernandes, Y. Beyad, R. Burns, G. Puxty, and M. Maeder, 'Reactions of CO<sub>2</sub> with Aqueous Piperazine Solutions: Formation and Decomposition of Mono- and Dicarbamic Acids/Carbamates of Piperazine at 25.0 ° C', 2013.
- [36] S. A. Freeman, R. Dugas, D. Van Wagener, T. Nguyen, and T. Gary, 'Energy Procedia Carbon dioxide capture with concentrated, aqueous



- piperazine', *Energy Procedia*, vol. 1, no. 1, pp. 1489–1496, 2009, doi: 10.1016/j.egypro.2009.01.195.
- [37] A. Haghtalab, M. Mohammadi, and Z. Fakhroueian, 'Absorption and solubility measurement of CO<sub>2</sub> in water based ZnO and SiO<sub>2</sub> nanofluids', Elsevier B.V., 2015, doi: 10.1016/j.fluid.2015.02.012.
- [38] P. S. Kumar, J. A. Hogendoorn, P. H. M. Feron, and G. F. Versteeg, 'New absorption liquids for the removal of CO<sub>2</sub> from dilute gas streams using membrane contactors', vol. 57, pp. 1639–1651, 2002.
- [39] V. Y. Dindore and G. F. Versteeg, 'Gas – liquid mass transfer in a cross-flow hollow fiber module: Analytical model and experimental validation', vol. 48, pp. 3352–3362, 2005, doi: 10.1016/j.ijheatmasstransfer.2005.03.002.
- [40] X. Fang, Y. Xuan, Q. Li, X. Fang, Y. Xuan, and Q. Li, 'Experimental investigation on enhanced mass transfer in nanofluids Experimental investigation on enhanced mass transfer in nanofluids', vol. 203108, no. May 2013, pp. 7–10, 2009, doi:

DOI: <https://doi.org/10.15379/ijmst.v10i3.1959>

This is an open access article licensed under the terms of the Creative Commons Attribution Non-Commercial License (<http://creativecommons.org/licenses/by-nc/3.0/>), which permits unrestricted, non-commercial use, distribution and reproduction in any medium, provided the work is properly cited.